Sorption Characteristics of Arsenic(V) for Removal from Water Using Agglomerated Nanostructure Iron(III)−Zirconium(IV) Bimetal Mixed Oxide

Kaushik Gupta, Tina Basu, and Uday Chand Ghosh*

Department of Chemistry, Presidency College, 86/1 College Street, Kolkata-700073, India

Arsenic(V) sorption reaction with nanostructured hydrous iron(III)−zirconium(IV) bimetal mixed oxide (NHIZO) was investigated experimentally with varying parameters, viz., the effects of pH, contact time, and isotherm equilibrium at (303 ± 1.6) K. The optimum pH estimated ranged between 5.0 and 7.0. The kinetic and equilibrium data (pH 7.0 ± 0.2) described the pseudosecond order and the Langmuir isotherm equations well, respectively. The Langmuir monolayer capacity estimated was (9.3582 ± 0.3116) $\mathrm{mg \cdot g^{-1}}$. Thermodynamics analysis of the data of isotherm equilibrium suggested the endothermic and spontaneous nature of the sorption reaction, and the latter took place with the increase of entropy ($\Delta S^0 = +96.6087$ $\mathrm{J \cdot mol^{-1} \cdot K^{-1}}$). The estimation of sorption energy ($E = 12.4700$ $\mathrm{kJ \cdot mol^{-1}}$) from the Dubinin−Radushkevich (D−R) isotherm analysis had suggested chemisorption of arsenic(V) on NHIZO.

1. Introduction

Arsenic, a toxic element, exists at four major oxidation states (−3, 0, +3, and +5). Occurrences of arsenic in some spring- and groundwaters are widespread,[1] which are used as the main sources for drinking by the countrymen of many underdeveloped countries like India and Bangladesh. Thus, important health issues result from arsenic levels in major drinking water resources above recommended WHO concentration (0.01 $\mathrm{mg \cdot dm^{-3}}$).[2] Arsenic mainly reaches humans through the drinking water where it mostly occurs at +3 and +5 forms, depending on the Eh and pH conditions.[3,4] This indicates the requirement of suitable arsenic contaminated water treatment technology for the countries where the supply of treated surface water in the remote villages is impossible in the near future because large funds are required for the technological shift. Consequently, several methods such as oxidation−precipitation, coagulation/electrocoagulation/precipitation, membrane filtration, surface sorption, and ion exchange etc. have been reported.[1,4−6] However, the surface sorption method has been found to be an alternative option for the treatment of high arsenic groundwater and is well accepted by the rural people of underdeveloped countries like India and Bangladesh for simple operation and low recurring cost. Numerous sorbent materials,[4,7] viz., activated carbon, agricultural products and byproducts, biomasses, and metal oxides or metal ion loaded biomaterials have been tested for the treatment of high arsenic contaminated ground-/wastewater and industrial effluents. The solid inorganic materials used in the bulk phase for arsenic removal from the aqueous solution are mostly the different mineralogical forms of iron(III)/aluminum(III) oxide and hydroxide,[4−19] mixed rare earth oxide,[20] and Ce(IV) doped iron oxide.[21] Some polyvalent metal oxides have been synthesized and tested for the arsenic sorption/removal in our laboratory.[22−27] Studies in recent years show the use of nanoscale zerovalent iron,[28,29] nanocrystalline titanium oxide,[30,31] and nanostructured akaganeite[32] for arsenic sorption from the aqueous solution which has encouraged us in undertaking work with the synthetic nanostructured Fe(III)-based hydrous mixed metal oxide materials. On this basis, nanostructured hydrous iron(III)−titanium(IV) mixed oxide has been synthesized and studied for arsenic removal.[33] The synthesis, characterization, and arsenic(III) sorption behavior of nanostructure hydrous iron(III)−zirconium(IV) bimetal mixed oxide (NHIZO) has also been reported.[34] In extension of our previous work,[34] NHIZO has been used systematically for arsenic(V) sorption from the aqueous solution for removal.

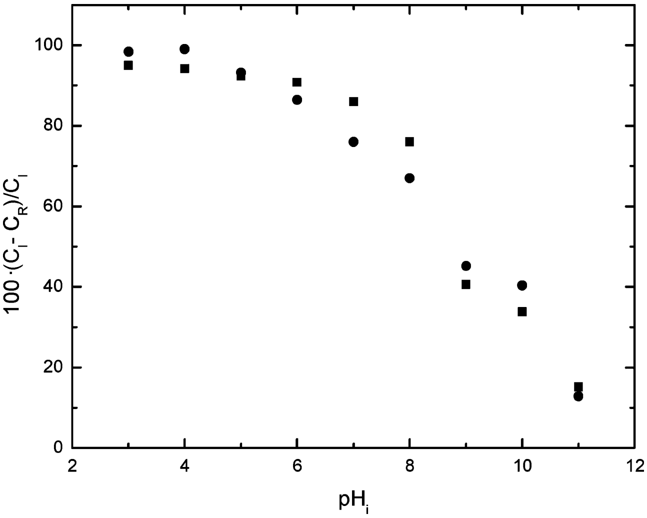

Figure 1. Effect of initial solution pH ($\mathrm{pH_i}$) on arsenic(V) sorption by NHIZO at T = (303 ± 1.6) K. C_I = ●, 5 $\mathrm{mg \cdot dm^{-3}}$; ■, 10 $\mathrm{mg \cdot dm^{-3}}$. The symbols represent the experimental data.

Thus, the present work reports herein the arsenic(V) sorption on NHIZO with varying solution pH, contact time for the rate and equilibrium for isotherm, and thermodynamics of the reaction.

2. Material and Methods

2.1. Chemicals. All chemicals used in the study were of guaranteed reagent (G. R., E. Merck, India) except disodium

---

* Corresponding author. Telephone/Fax: +91-33-2241 3893. E-mail: ucghosh@yahoo.co.in.

10.1021/je900282m CCC: $40.75

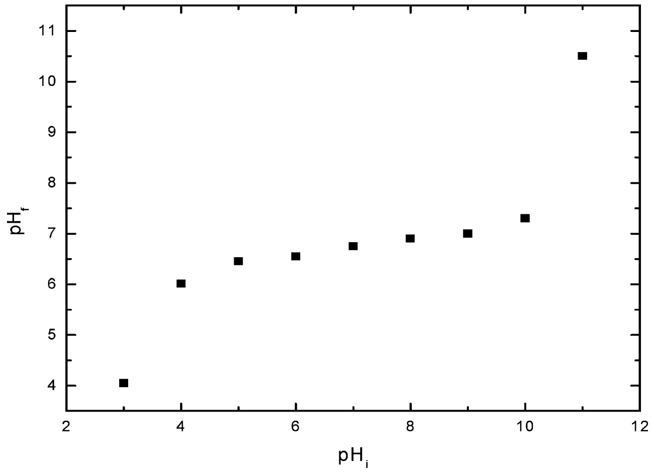

Figure 2. Variation of equilibrium solution pH (pH_f) as a function of initial solution pH (pH_i) for arsenic(V) sorption by NHIZO at $T = (303 \pm 1.6)$ K. The symbols represent the experimental data.

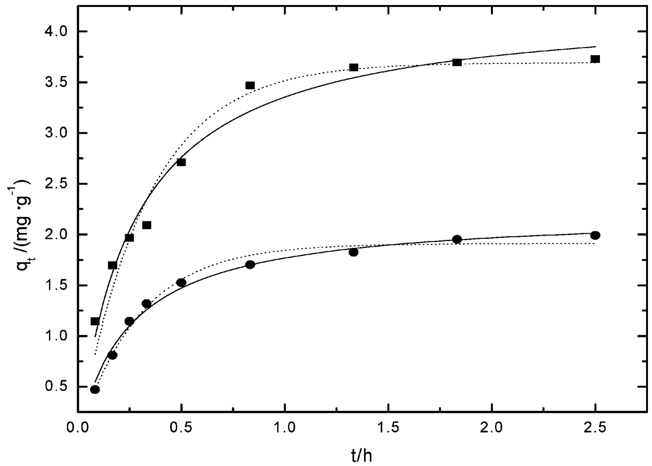

Figure 3. Sorption kinetics of arsenic(V) on NHIZO at different initial arsenic(V) concentrations ($T = (303 \pm 1.6)$ K, $pH_i = 7.0 \pm 0.2$). ●, 5 $mg \cdot dm^{-3}$; ■, 10 $mg \cdot dm^{-3}$; -----, pseudofirst order; —, pseudosecond order. The symbols represent the experimental data, and the lines predicted the model fits.

hydrogen arsenate (Na_2HAsO_4) (99.9 %, Aldrich, USA), anhydrous ferric chloride ($FeCl_3$) (98 %, laboratory reagent, E. Merck, India), sodium hydroxide (NaOH) (98 %, laboratory reagent, SD Fine Chemicals, India), and zirconium oxychloride octahydrate ($ZrOCl_2$, $8H_2O$) (35.5 % as ZrO_2, ordinary grade, Loba Chemie, India).

2.2. Arsenic(V) Solutions. A standard stock arsenic(V) solution (1000 $mg \cdot dm^{-3}$) was prepared by dissolving 2.08 g of Na_2HAsO_4 in arsenic-free distilled water (1.0 dm^3) into a volumetric flask. The arsenic(V) solutions of required concentrations for working were made by diluting the stock with 0.2 % (v/v) HCl. The stock solution was prepared afresh after every 15 days.

2.3. Arsenic Analysis. Arsenic in solution was analyzed by a hydride generator atomic absorption spectrophotometer (Perkin-Elmer Aanalyst 200) (detection limit: 0.01 μg, accuracy > 90 %) and a UV−vis spectrophotometer (Hitachi model 3210) (detection limit: 1.0 μg, accuracy > 90 %) using the methods as described by AWWA, APHA, and WEF.[35]

2.4. Synthesis of NHIZO. The procedure used for the material synthesis had been reported in the previous communication.[34] The outline of the procedure used for the NHIZO synthesis was the hydrolysis (pH to ~6.0) of hot (~60 °C) well-mixed (speed: 250 rpm) ferric chloride (0.18 M $FeCl_3$ in 0.1 M HCl) and zirconium oxychloride (0.02 M $ZrOCl_2$ in 0.1 M HCl) (v/v = 1:1) solution with 1.0 M sodium hydroxide. The aged (48 h) brown precipitate was filtered, washed three times with deionized water, and dried (~80 °C) in the air-oven. The dried mass when treated with cold water gave the agglomerated particles of size ranging from (140 to 290) μm for use in the experiments.

2.5. Batch Experiments. 2.5.1. pH Effect. The experiment for estimating the influence of initial solution pH (pH_i) on solute sorption by the sorbent was carried out by mixing 0.1 g of NHIZO with 0.05 dm^3 of arsenic(V) solution (concentration: (5.0 or 10.0) $mg \cdot dm^{-3}$), adjusted at pH_i ranging from 3.0 to 11.0, into the separate PET bottles (0.25 dm^3). The reaction mixtures of PET bottles were agitated (speed: (280 ± 5) rpm) for 2.0 h. The pH (pH_f) of the agitated reaction mixture was recorded by immersing a pH-meter (model LI-127, ELICO, India) electrode. The residual arsenic in the filtered sample solution was analyzed.[35]

2.5.2. Sorption Kinetics. The batch method was used for kinetics of arsenic(V) sorption by NHIZO at pH_i 7.0 ± 0.2 and temperature (303 ± 1.6) K. Here, 0.5 dm^3 of arsenic solution (concentration: (5.0 or 10.0) $mg \cdot dm^{-3}$) was taken with 1.0 g of NHIZO into a 1.0 dm^3 glass vessel and placed in a thermostat bath to attain the desired temperature. Thereafter, the reaction mixture was agitated [(280 ± 5) rpm] using a speed adjustable agitator. A pH-meter electrode was inserted into the solutions 10 min before withdrawing of samples for pH measurement, and 0.1 M NaOH or 0.1 M HCl was added, if required, for pH adjustment (~7.0) during an experimental run. A measured volume of the reaction mixture, 0.002 dm^3 at the initial three stages and 0.005 dm^3 in the later stages, was sampled at a definite time interval until the equilibrium was reached. The sample solutions were filtered using 0.45 μm membrane filters, and the filtrates were analyzed for residual arsenic.[35]

2.5.3. Sorption Isotherm. Batch sorption isotherm experiments were conducted at a temperature (303 ± 1.6) K and at pH_i 7.0 ± 0.2. Here, arsenic(V) solutions of concentration ranged from (5.0 to 150.0) $mg \cdot dm^{-3}$ and adsorbent doses of 2 $g \cdot dm^{-3}$ were used. The agitation (speed: (280 ± 5) rpm) time used was 2.0 h. The solution pH was adjusted twice in the middle (at 1.0 h and 1.5 h of agitations from zero time) using 0.1 M HCl and/or 0.1 M NaOH as required. Residual arsenic was determined in the filtered sample.[35]

Table 1. Values of Kinetic Equation Parameters Estimated for the Sorption Arsenic(V) by NHIZO ($pH_i = 7.0 \pm 0.2$, $T = (303 \pm 1.6)$ K)[a]

	pseudo-first order				pseudo-second order			
arsenic(V)concentration	k_1	q_e			k_2	q_e		
($mg \cdot dm^{-3}$)	(h^{-1})	($mg \cdot g^{-1}$)	R^2	χ^2	($g \cdot mg^{-1} \cdot h^{-1}$)	($mg \cdot g^{-1}$)	R^2	χ^2
5.0	3.3715 ± 0.1931	1.9096 ± 0.0341	0.9882	0.0038	1.7841 ± 0.1718	2.2151 ± 0.0485	0.9905	0.0030
10.0	3.0296 ± 0.2825	3.6924 ± 0.1106	0.9674	0.0366	0.8559 ± 0.1299	4.2702 ± 0.1504	0.9760	0.0270

[a] The value after the ± sign gives the standard deviation.

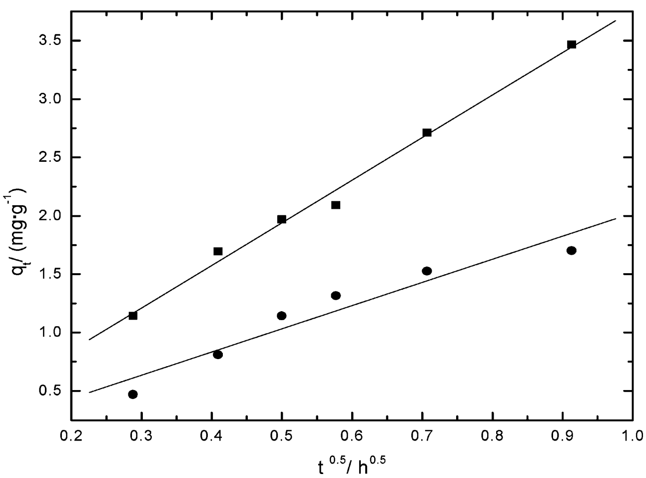

Figure 4. Variation of arsenic(V) sorption capacity of NHIZO as a function of square root of time at $T = (303 \pm 1.6)$ K and $pH_i = 7.0 \pm 0.2$. C_I = ●, 5 mg·dm^{-3}; ■, 10 mg·dm^{-3}. The symbols represent the experimental data, and the lines are the linear fits.

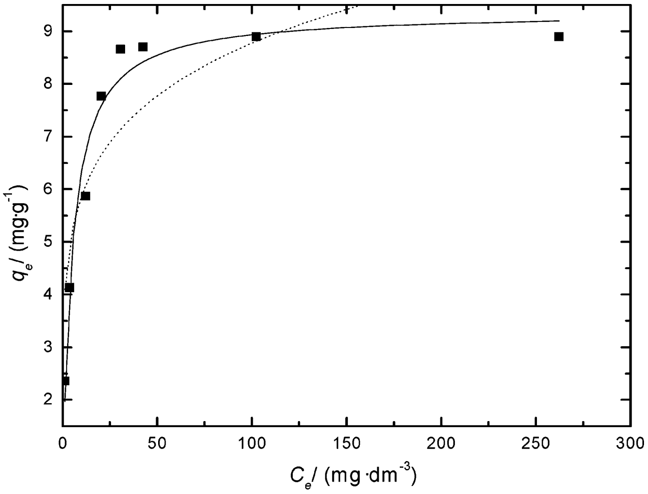

Figure 5. Equilibrium data for arsenic(V) sorption by NHIZO at $T = (303 \pm 1.6)$ K and at $pH_i = 7.0 \pm 0.2$. ---, Fruendlich; —, Langmuir. The symbols represent the experimental data, and the lines predicted the model fit.

2.5.4. Calculation of Uptake Capacity. Arsenic(V) uptake capacity, q_e (or q_t), at equilibrium (or at time, t) of NHIZO was calculated from the following mass balance relation

$$q_e \text{ (or } q_t) = (C_I - C_R)\cdot(V/W)$$

where C_I and C_R are, respectively, the initial and residual concentration (mg·dm^{-3}) of arsenic in solution and V and W are the test solution volume (dm^3) and mass (g) of sorbent, respectively, used for the test.

3. Results and Discussion

3.1. Characterization of the Material. The characterization of this agglomerated material was reported[34] by the X-ray powder diffraction (XRD), scanning electron microscopy (SEM), transmission electron microscopy (TEM), Föurier transform infrared (FTIR) spectroscopy, and thermal and surface area analyzes. It was recorded that the material was hydrated and crystalline with agglomerated surface morphology. The crystallite particle size as obtained from TEM image analysis ranged between (16 and 21) nm. The analyzed specific surface area and pH_{zpc} of the material were found to be 263 m^2·g^{-1} and 6.8 ± 0.2, respectively.

3.2. pH Effect. Figure 1 demonstrates the effect of initial solution pH (pH_i) on arsenic(V) sorption by NHIZO at (303 ± 1.6) K, and that indicated the pH-sensitive sorption reaction of arsenic(V). It was found that the agitated solution pH (pH_f) had increased with respect to the pH_i up to near pH_{zpc} (= 6.8 ± 0.2)[34] and noted that it decreased at above pH_{zpc} (Figure 2) of the material. At pH_i ranging from 3.0 to 5.0, the arsenic(V) removal percentage ranged between (95.0 and 99.0). The result obtained was found to be different from that reported by Kundu and Gupta[5] but nearly similar to the results of Lakshmipathiraj et al.[36] Too high removal percentage in the said pH range is due to either the Columbic attraction between positive surface of the solid (R1) and $H_2AsO_4^-$ ($pK_a^1 = 2.19$) or the ligand-exchange phenomenon.

$$MOH_{(s)} + H^+_{(aq)} \rightarrow MOH^+_{2(s)} \quad (pH < pH_{zpc}) \qquad (R1)$$

Whatever the reaction mechanism, the increase of pH_f value of the solution was indicated. Nearly the same arsenic(V) sorption percentage for the solute loads studied in the pH_i range between 3.0 and 5.0 is presumably due to (i) the presence of excess active surface sites compared to the solute loads added and (ii) $pH_f < pH_{zpc}$. Arsenic(V) sorption percentage was found to decrease slightly from pH_i 5.0 to 7.0, and pH_f was near/around pH_{zpc}. This is presumably due to the decrease of Columbic attraction between near neutral/neutral solid surface and $H_2AsO_4^-$ species. The sorption percentage had decreased to a slightly greater extent at pH_i from 7.0 to 8.0 than that at pH_i 6.0 to 7.0 which was noted clearly for the case of solute load of 10.0 mg·dm^{-3}, and that was not so significant for the solute load of 5.0 mg·dm^{-3}. The latter might be due to the low solute/solid ratio. Arsenic(V) sorption percentage decreased sharply at $pH_i \geq 8.0$, which is mainly due to (i) the negative surface of solid (R2) as the solution pH_f was greater than the pH_{ZPC} value (Figure 2) and (ii) the presence of dinegative

$$MOH_{(s)} \rightarrow MO^-_{(s)} + H^+_{(aq)} \quad (pH > pH_{zpc}) \qquad (R2)$$

arsenic(V) species (pK_a^2 of $H_3AsO_4 = 6.94$) in solution. Thus, the solute species experience strong Columbic repulsion before sorption when it comes at the boundary layer of the solid surface and liquid phase.

3.3. Kinetic Analysis. Figure 3 demonstrates the kinetic data of arsenic(V) sorption by NHIZO obtained at pH_i 7.0 (± 0.2) and temperature 303 (± 1.6) K. It was found that ~75 % of total sorbed arsenic(V) took place in 0.5 h, and the time taken to reach the equilibrium was ~1.6 h.

These data (Figure 3) have been analyzed by the nonlinear least-squares fit method using the appropriate coordinate of each equation by the pseudofirst order[37] (eq 1) and the pseudosecond order[38] (eq 2) kinetic equations, and the fits are shown with the experimental data in Figure 3.

$$\log(q_e - q_t) = \log q_e - (k_1\cdot t)/2.303 \qquad (1)$$

$$t/q_t = 1/(k_2\cdot q_e^2) + t/q_e \qquad (2)$$

where q_e and q_t are the sorption capacities (mg·g^{-1}) at equilibrium and at any time, t (h), respectively; and k_1 (h^{-1}) and k_2 (g·mg^{-1}·h^{-1}) are the rate constants, respectively, related to eqs 1 and 2. The kinetic parameters estimated from the computer spreadsheet of the nonlinear plots for the used kinetic equations are shown in Table 1. The χ^2 values estimated for the solute solution of concentrations (5.0 and 10.0) mg·dm^{-3}, respectively, from the analysis of the pseudosecond order equation (eq 2) were 0.0030 and 0.0270, while those from the pseudofirst order equation (eq 1) were 0.0038 and 0.0366. The

Table 2. Values of Isotherm Equation Parameters Estimated by the Nonlinear Analysis of Equilibrium Arsenic(V) Sorption Data on NHIZO ($pH_i = 7.0 \pm 0.2$, $T = (303 \pm 1.6)$ K)[a]

Isotherm Parameters							
Langmuir				Freundlich			
		q_m	K_a			K_F	
R^2	χ^2	$mg \cdot g^{-1}$	$dm^3 \cdot g^{-1}$	R^2	χ^2	$(mg \cdot g^{-1})(dm^3 \cdot mg^{-1})^{-1/n}$	n
0.9670	0.2372	9.3582 ± 0.3116	0.2107 ± 0.0370	0.7574	1.7971	3.9254 ± 0.7469	5.7263 ± 1.5221

[a] The value after the ± sign gives the standard deviation.

Table 3. Comparison of the Langmuir Monolayer Arsenic(V) Sorption Capacity ($q_m/mg \cdot g^{-1}$) with Some Reported Sorbent Materials

adsorbent	q_m $(mg \cdot g^{-1})$	ref	asenic(V) concentration $mg \cdot dm^{-3}$ and pH
red mud	0.514	11	33.37 to 400.4/$\mu mol \cdot dm^{-3}$
iron oxide coated sand	0.043	15	100/$\mu g \cdot dm^{-3}$ and 7.6
granular ferric oxide	8.5	9	5 to 100 and 8 to 9
ferrihydrite	111.02	10	0.267 to 26.7/$mmol \cdot dm^{-3}$
activated alumina	15.9	13	2.85 to 11.5 and 5.2
hydrous stannic oxide	4.3	25	1.0 to 10 and 7.0
crystalline ferric oxide	25.0	22	50.0 to 250.0 and 3.0 to 4.0
hydrous zirconium oxide	31.0 to 32.0	24	50.0 to 250.0 and 2.0 to 3.0
nanohydrous iron−titanium mixed oxide	14.3	33	5 to 150 and 7.0
mixed rare earth oxide	2.95	20	50.0 and 6.5
nanostructured akaganeite	1.80	32	5 to 20 and 7.5
iron oxide coated biomass	0.059	42	up to 100/$\mu g \cdot dm^{-3}$ and 6.0
NHIZO	9.36	present work	5.0 to 150 and 7.0

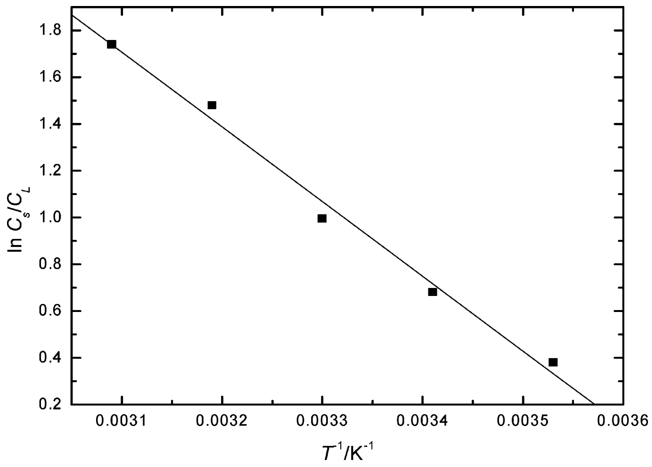

Figure 6. Variation of ln C_s/C_L as a function of $1/T$ of arsenic(V) sorption by NHIZO at $pH_i = 7 \pm 0.2$. The symbol represents the experimental data, and the line is the linear fit.

R^2 (regression coefficient) values estimated for the aforesaid solute concentrations from the pseudosecond order equation (eq 2) were 0.9905 and 0.9760, and those from the pseudofirst order (eq 1) were 0.9882 and 0.9674. Thus, based on the estimated χ^2 and correlation coefficient (R^2) values, it could be generalized that the experimental data described the pseudosecond order equation (eq 2) well and better than the pseudofirst order equation (eq 1). The pseudosecond order rate constant (k_2, $g \cdot mg^{-1} \cdot h^{-1}$) value has been found to decrease with increasing initial arsenic(V) load in solution per gram of NHIZO. This is presumably due to the initial more rapid growing of surface negative charge for fast sorption of arsenic(V) on the exterior surface of the solid from the concentrated (10.0 $mg \cdot dm^{-3}$) solute solution than from the dilute (5.0 $mg \cdot dm^{-3}$) which inhibits the later stages of sorption at the interior surface of solid by Columbic repulsion between like charges on solid surface and the solute species in solution. This indicates very slow sorption at the later stages, and the estimated overall k_2 value was less for the solute solution of higher concentration than that for the case of solute solution of the lower one. Thus, the arsenic(V) sorption is kinetically more favorable from the solution of lower solute load than from the higher one.

The rate-determining step (RDS) of the surface sorption reaction can be ascertained from the Weber−Morris[39] plot for the equation (eq 3)

$$q_t = k_{id} \cdot t^{0.5} \tag{3}$$

where k_{id} is sorption constant ($mass \cdot g^{-1} \cdot time^{-0.5}$), and the other terms have been described elsewhere. If the plot of q_t versus $t^{0.5}$ is a straight line with intercept zero, then RDS is intraparticle diffusion, and if the plot has some intercept value, the RDS should be a multistage one. For the present case, the plots (Figure 4) show a straight line with some intercept value, which indicates the RDS is not controlled by the intraparticle diffusion phenomenon only. Instead, it should be the multistage controlled process.

3.4. Isotherm Analysis. Figure 5 demonstrates the equilibrium data for the arsenic(V) sorption on NHIZO obtained at the temperature 303 (± 1.6 K) at pH 7.0 (± 0.2). To evaluate the nature of the sorption reaction, the following most commonly used isotherm model equations were used for the data analysis

$$\text{Langmuir isotherm:}^{40}\ q_e = (q_m \cdot K_a \cdot C_e)/(1 + K_a \cdot C_e) \tag{4}$$

$$\text{Freundlich isotherm:}^{41}\ q_e = K_F \cdot C_e^{(1/n)} \tag{5}$$

where C_e ($mg \cdot dm^{-3}$) and q_e ($mg \cdot g^{-1}$) are, respectively, the equilibrium concentration and capacity. q_m and K_a are the Langmuir constants related to monolayer sorption capacity ($mg \cdot g^{-1}$) and sorption equilibrium constant ($dm^3 \cdot g^{-1}$), respectively. K_F and n are the Freundlich constants related to sorption capacity $(mg \cdot g^{-1})(dm^3 \cdot mg^{-1})^{-1/n}$ and intensity, respectively.

The isotherm data shown as points (Figure 5) had been analyzed with the aforesaid equations (eqs 4 and 5) by the nonlinear methods using the origin software spreadsheet, and the fits of data are also shown in Figure 5. The related isotherm parameters evaluated from the nonlinear analyses of the data are given in Table 2. On the basis of either the statistical error

Table 4. Values of Thermodynamic Parameters Evaluated for Arsenic(V) Sorption by NHIZO ($\text{pH}_i = 7.0 \pm 0.2$, $T = (303 \pm 1.6)$ K)

arsenic(V) concentration	ΔH^0	ΔS^0	$-\Delta G^0/(\text{kJ}\cdot\text{mol}^{-1})$				
$(\text{mg}\cdot\text{dm}^{-3})$	$(\text{kJ}\cdot\text{mol}^{-1})$	$(\text{J}\cdot\text{mol}^{-1}\cdot\text{K}^{-1})$	283 K	293 K	303 K	313 K	323 K
10.0	+26.5715	+96.6087	0.7688	1.7349	2.7009	3.6670	4.6331

chi-square (χ^2) or the linear regression coefficient (R^2) values (Table 2), it could be said that the fits of the present equilibrium data are found better with the Langmuir isotherm (eq 4) than the Freundlich (eq 5). The Langmuir monolayer sorption capacity (q_m, $\text{mg}\cdot\text{g}^{-1}$) value obtained from the nonlinear method of analysis was 9.3582 (± 0.31116) $\text{mg}\cdot\text{g}^{-1}$. To estimate the arsenic(V) removal efficiency of NHIZO, the q_m value has been compared with some reported data for different sorbents in Table 3. As the q_m value of the sorbent varies with the initial concentration range of the solute, pH, and other experimental conditions, it becomes difficult to compare directly. However, it could be predicted from the comparison table (Table 3) that NHIZO is a fairly good scavenging agent for arsenic(V) at normal conditions compared to many other sorbents.

3.5. Thermodynamic Parameters. Thermodynamic parameters for the present sorption reaction were calculated using the standard relations available in the literature[43] and the data shown as points in Figure 5. The values of the standard enthalpy change (ΔH^0) and the standard entropy change (ΔS^0) were estimated from the plot ($\ln C_s/C_L$ versus $1/T$) shown in Figure 6, which are given in Table 4. The ΔH^0 for the present reaction was found to be positive (+26.5715 $\text{kJ}\cdot\text{mol}^{-1}$), which proves the endothermic nature of the sorption reaction. The ΔS^0 of the process was found to be positive (+96.6087 $\text{J}\cdot\text{mol}^{-1}\cdot\text{K}^{-1}$), which indicates the increase of randomness at the solid−liquid interface when the solute sorption took place on the solid. This is presumably due to the increase of released solvent molecules when solvated solute distributes on the solid phase from the aqueous solution and the number of molecules increases at the solid−liquid interface. The results obtained are found to be similar to those that had been reported previously.[5,33,34] The standard Gibbs free energy change (ΔG^0) was found to be negative, and the value increased with increasing temperature (Table 4). This suggests the spontaneous nature of the sorption reaction at the temperatures studied, and the reaction spontaneity increases with increasing temperature, which is characteristic of an endothermic surface reaction.

3.6. Energy of Sorption. The equilibrium isotherm data shown as points in Figure 5 have been analyzed by the Dubinin−Radushkevich (D−R) equation[44] (eq 6) to evaluate the sorption energy.

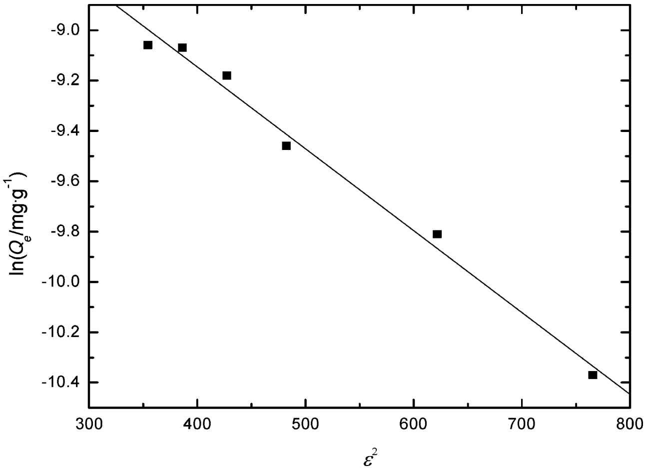

Figure 7. Dubinin−Radushkevich isotherm plot of arsenic(V) sorption on NHIZO at $T = (303 \pm 1.6)$ K and $\text{pH}_i = 7.0 \pm 0.2$. The symbol represents the experimental data, and the line is the fit of data.

Table 5. Values of the Dubinin−Radushkevich (D−R) Isotherm Parameters Evaluated for Arsenic(V) Sorption by NHIZO ($\text{pH}_i = 7.0 \pm 0.2$, $T = (303 \pm 1.6)$ K)[a]

D−R isotherm parameters			
	E	K_{DR}	Q_m
R^2	$(\text{kJ}\cdot\text{mol}^{-1})$	$(\text{mol}^2\cdot\text{kJ}^{-2})$	$(\text{mol}\cdot\text{kg}^{-1})$
0.9946	12.4700	0.0023 ± 0.0311	0.0004

[a] The value after the ± sign gives the standard deviation.

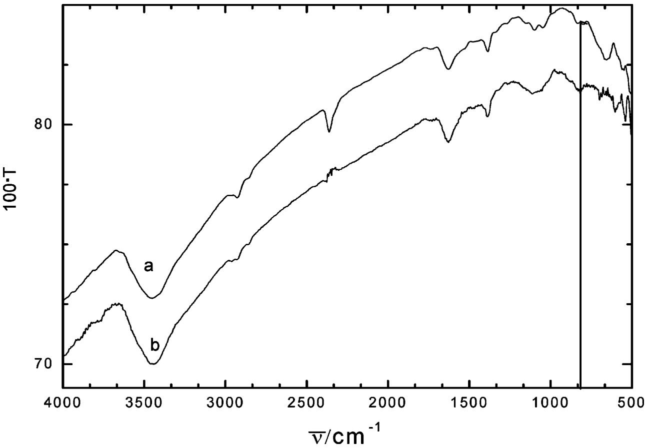

Figure 8. Föurier transform infrared (FTIR) spectra of (a) NHIZO and (b) As(V)-sorbed NHIZO.

$$\ln Q_e = \ln Q_m - K_{DR}\cdot\varepsilon^2 \tag{6}$$

where Q_e and Q_m are the equilibrium and saturated sorption capacities in $(\text{mol}\cdot\text{kg}^{1-})$, respectively, and K_{DR} is a constant related to the free energy ($\text{mol}^2\cdot\text{kJ}^{-2}$) of sorption. ε, the Polanyi potential, is expressed by the equation below (eq 7)

$$\varepsilon = RT\ln\{1 + (1/C_e)\} \tag{7}$$

where C_e has its usual meaning described elsewhere; R and T, respectively, are the molar gas constant and absolute temperature. The Q_m and K_{DR} parameters, respectively, were evaluated from the intercept and slope of the plot of $\ln Q_e$ versus ε^2 (Figure 7), and the values are shown in Table 5. If the mean energy (E, $\text{kJ}\cdot\text{mol}^{-1}$) of sorption, which can be calculated by computation of K_{DR} ($\text{kJ}\cdot\text{mol}^{-1}$) in the following relation (eq 8), ranges from 8.0 to 16.0, the sorption should be of chemical nature.

$$E = (-2K_{DR})^{-0.5} \tag{8}$$

The mean sorption energy (E) value calculated at studied temperature is shown also in Table 5. The E-value ($\text{kJ}\cdot\text{mol}^{-1}$) for the present reaction was found to be 12.47, which ranged between (8.0 and 16.0) $\text{kJ}\cdot\text{mol}^{-1}$. This indicates the chemisorption of arsenic(V) on NHIZO, which is similar to the result that had been reported by some other authors[5,12] but somewhat different from our previous result.[33] Thus, the plausible mechanism of arsenic(V) adsorption by NHIZO at pH_i 7.0 (± 0.2) can be depicted as

$$\text{M}-\text{OH} + \text{H}_2\text{AsO}_4^{-}\text{Na}^{+} \overset{\text{pH} \sim 7.0}{\rightleftharpoons} \text{M}-\text{OAsO}_2(\text{OH})^{-}\text{Na}^{+} + \text{H}_2\text{O}$$

The mechanism suggested is supported by the fact that the pH_i (7.0 ± 0.2) and pH_f (after arsenic(V) sorption) remained nearly close with each other.

To confirm the mechanism suggested, FTIR spectra of NHIZO and As(V)−NHIZO were analyzed. Both spectra (Figure 8) showed absorption peaks at wavenumbers (cm^{-1}) around 3450 and 1620, respectively, for the stretching and bending modes of O−H bonds. The peak at 2300 cm^{-1} for the spectra of NHIZO was for the C−O stretching mode of CO_3^{2-}, which has presumably come from the alkali used for the preparation. The peak at wavenumber around 895 cm^{-1} observed for the spectra of arsenic(V)−NHIZO was the stretching vibration mode of the As−O bond in AsO_4^{3-}.[36] The broad peak at ~650 cm^{-1} of NHIZO was presumably for the vibration mode of the M−O bond which is found to disappear in the spectra of arsenic(V)−NHIZO, and instead two peaks appear at (~600 and 670) cm^{-1} in the latter spectra. These may be due to the formation of the M−O−As (HAsO_4^{2-}) bond in place of M−OH in arsenic(V)−NHIZO.

4. Conclusion

- Agglomerated nanostructured synthetic bimetal mixed iron(III)−zirconium(IV) oxide (NHIZO) shows good sorption affinity for arsenic(V) in a wide range of initial solution pH (pH_i 3.0 to 7.0).
- The sorption reaction takes ~1.6 h to attain the equilibrium.
- The kinetic data for the sorption reaction describe the pseudosecond order equation better than the pseudofirst order equation.
- The sorption pattern of arsenic(V) by NHIZO fits well to the Langmuir model. The Langmuir capacity q_m [(9.3582 ± 0.3116) $\text{mg} \cdot \text{g}^{-1}$] is higher than many of the conventional sorbents for arsenic.
- The reaction is endothermic ($\Delta H^0 = +26.5715\ \text{kJ} \cdot \text{mol}^{-1}$), and that takes place with increasing entropy ($\Delta S^0 = +96.6087\ \text{J} \cdot \text{mol}^{-1} \cdot \text{K}^{-1}$).
- The increasingly negative Gibbs free energy change ($-\Delta G^0 = (0.7688 \text{ to } 4.6331)\ \text{kJ} \cdot \text{mol}^{-1}$) indicates the increase of reaction spontaneity with temperature.
- Arsenic(V) sorption reaction with NHIZO is a chemisorption phenomenon.

Acknowledgment

The authors are thankful to the Head, Department of Chemistry, and the Principal, Presidency College, Kolkata, India, for laboratory facilities.

Literature Cited

(1) Smedley, P. L.; Kinniburgh, G. A review of the source, behaviour and distribution of arsenic in natural waters. *Appl. Geochem.* **2002**, *17*, 517–568.

(2) Vaughan, D. J. Arsenic. *Elements* **2006**, *2*, 71–75.

(3) Lorenzen, L.; Van Deventer, J. S. J.; Landi, W. M. Factors affecting the mechanism of the adsorption of arsenic species on activated carbon. *Miner. Eng.* **1995**, *8*, 557–569.

(4) Mohan, D.; Pittman, C. U., Jr. Arsenic removal from water/wastewater using adsorbents- a critical review. *J. Hazard. Mater.* **2007**, *142*, 1–53.

(5) Kundu, S.; Gupta, A. K. Investigation on the Adsorption Efficiency of Iron Oxide Coated Cement (IOCC) towards As(V) − Kinetics, Equilibrium and Thermodynamics Studies. *Colloid Surf. A: Physiochem. Eng. Aspects* **2006**, *273*, 121–128.

(6) Kundu, S.; Gupta, A. K. Adsorption Characteristic of As(III) from Aqueous Solution on Iron Oxide Coated Cement (IOCC). *J. Hazard. Mater.* **2007**, *142*, 97–104.

(7) Mondal, P.; Majumder, C. B.; Mohanty, B. Laboratory Based Approaches for Arsenic Remediation from Contaminated Water: Recent Developments. *J. Hazard. Mater.* **2006**, *B137*, 464–479.

(8) Wilkie, J. A.; Hering, J. G. Adsorption of Arsenic onto Hydrous Ferric Oxide: Effects of Adsorbate/Adsorbent Ratios and Co-occurring Solutes. *Colloids Surf., A: Physico. Eng. Aspects* **1996**, *107*, 97–110.

(9) Driehaus, W.; Jekel, M.; Hilderbrandt, U. Grannular Ferric Hydroxide-a New Adsorbent for the Removal of Arsenic from Natural Water. *J. Water Supply: Res. Technol.−AQUA* **1998**, *47*, 30–35.

(10) Raven, K. P.; Jain, A.; Loeppert, R. H. Arsenite and Arsenate Adsorption on Ferrihydrite: Kinetics, Equilibrium, and Adsorption Envelopes. *Environ. Sci. Technol.* **1998**, *32*, 344–349.

(11) Altundogan, H. S.; Altundogan, S.; Tumen, F.; Bildik, M. Arsenic Adsorption from Aqueous Solution by Activated Red Mud. *Waste Manage.* **2002**, *22*, 357–363.

(12) Singh, T. S.; Pant, K. K. Equilibrium, Kinetics and Thermodynamic Studies for Adsorption of As(III) on Activated Alumina. *Sep. Purif. Technol.* **2004**, *36*, 139–147.

(13) Lin, T. F.; Wu, J. K. Adsorption of Arsenite and Arsenate within Activated Alumina Grains: Equilibrium and Kinetics. *Water Res.* **2001**, *35*, 2049–2057.

(14) Katsoyiannis, I. A.; Zouboulis, A. I. Removal of Arsenic from Contaminated Water Sources by Sorptoin onto Iron Oxide-Coated Polymeric Materials. *Water Res.* **2002**, *36*, 5141–5155.

(15) Thirunavukkarasu, O. S.; Viraraghavan, T.; Subramanian, K. S. Arsenic Removal from Drinking Water using Iron Oxide Coated Sand. *Water, Air, Soil Pollut.* **2003**, *142*, 95–111.

(16) Zeng, L. Arsenic Adsorption from Aqueous Solution on an Fe(III)-Si Binary Oxide Adsorbent. *Water Qual. Res. J. Can.* **2004**, *39*, 269–277.

(17) Kuriakose, S.; Singh, T. S.; Pant, K. K. Adsorption of As(III) from Aqueous Solution onto Iron Oxide Impregnated Activated Alumina. *Water Qual. Res. J. Can.* **2004**, *39*, 260–268.

(18) Hlavay, J.; Polyak, K. Determination of Surface Properties of Iron Hydroxide-Coated Alumina Adsorbent for Removal of Arsenic from Drinking Water. *J. Colloid Interface Sci.* **2005**, *284*, 71–77.

(19) Lenoble, V.; Bouras, O.; Deluchat, V.; Serpaud, B.; Bollinger, J. C. Arsenic Adsorption onto Pillared Clays and Iron Oxides. *J. Colloid Interface Sci.* **2002**, *255*, 52–58.

(20) Raichur, A. M.; Penvekar, V. Removal of As(V) by Adsorption on to Mixed Rare Earth Oxides. *Sep. Sci. Technol.* **2002**, *37*, 1095–1108.

(21) Zhang, Y.; Yang, M.; Huang, X. Arsenic(V) Removal with a Ce(IV)-doped Iron Oxide Adsorbent. *Chemosphere* **2003**, *51*, 945–952.

(22) Manna, B. R.; Dey, S.; Debnath, S.; Ghosh, U. C. Removal of Arsenic from Ground Water using Crystalline Hydrous Ferric Oxide (CHFO). *Water Qual. Res. J. Can.* **2003**, *38*, 193–210.

(23) Manna, B. R.; Dasgupta, M.; Ghosh, U. C. Studies on Crystalline Hydrous Titanium Oxide (CHTO)- as Scavenger of Arsenic (III) from Natural Water. *J. Water Supply: Res. Technol.−AQUA* **2004**, *53*, 483–495.

(24) Manna, B. R.; Debnath, S.; Hossain, J.; Ghosh, U. C. Trace Arsenic-contaminated Groundwater Upgradation using Hydrated Zirconium Oxide (HZO). *J. Ind. Pollut. Control* **2004**, *20*, 247–266.

(25) Manna, B. R.; Ghosh, U. C. Adsorption of Arsenic from Aqueous Solution by Synthetic Hydrous Stannic Oxide. *J. Hazard. Mater.* **2007**, *144*, 522–531.

(26) Ghosh, U. C.; Bandhyopadhyay, D.; Manna, B. R.; Mandal, M. Hydrous Iron(III)-Tin(IV) Binary Mixed Oxide: Arsenic Adsorption Behaviour. *Water Qual. Res. J. Can.* **2006**, *41*, 198–209.

(27) Manna, B. R.; Ghosh, U. C. Pilot-Scale Performance of Arsenic and Iron Removal from Contaminated Groundwater. *Water Qual. Res. J. Can.* **2005**, *40*, 82–90.

(28) Kanel, S. R.; Manning, B.; Charlet, L.; Choi, H. Removal of Arsenic(III) from Groundwater by Nanoscale Zero-valent Iron. *Environ. Sci. Technol.* **2005**, *39*, 1290–1298.

(29) Yuan, C.; Lien, H.-L. Removal of Arsenate from Aqueous Solution using Nanoscale Iron Particles. *Water Qual. Res. J. Can.* **2006**, *41*, 210–215.

(30) Pena, M. E.; Korfiatis, G. P.; Patel, M.; Lippincott, L.; Meng, X. Adsorption of As(V) and As(III) by Nanocrystalline Titanium dioxide. *Water Res.* **2005**, *39*, 2327–2337.

(31) Jing, C.; Meng, X.; Liu, S.; Baidas, S.; Patraju, R.; Christodoulatos, C.; Korfiatif, G. P. Surface Complexation of Organic Arsenic on Nanocrystalline Titanium dioxide. *J. Colloid Interface Sci.* **2005**, *290*, 14–21.

(32) Deliyanni, E. A.; Bakoyannakis, D. N.; Zoubaulis, A. I.; Matis, K. A. Sorption of As(V) ion by Akaganeite Type Naocrystals. *Chemosphere* **2003**, *50*, 155–163.

(33) Gupta, K.; Ghosh, U. C. Arsenic Removal Using Hydrous Nanostructure Iron(III)-Titanium(IV) Binary Mixed Oxide from Aqueous Solution. *J. Hazard. Mater.* **2009**, *161*, 884–892.

(34) Gupta, K.; Biswas, K.; Ghosh, U. C. Nanostructure Iron(III)-Zirconium(IV) Binary Mixed Oxide: Synthesis, Characterization and Physicochemical Aspects of Arsenic(III) Sorption from the Aqueous solution. *Ind. Eng. Chem. Res.* **2008**, *47*, 9903–9912.

(35) *Standard Methods for the Examination of Water and Wastewater*, 20th ed.; Clesceri, L. S., Greenberg, A. E., Eaton, A. D., Eds.; American Public Health Association (APHA), American Water Works Association (AWWA), Water Environment Federation (WEF): Washington, DC, 1998; pp 4−82.

(36) Lakshmipathiraj, P.; Narasimhan, B. R. V.; Prabhakar, S.; Bhaskar Raju, G. Adsorption of Arsenate on Goethite from Aqueous Solutions. *J. Hazard. Mater.* **2006**, *B136*, 281–287.

(37) Lagergren, S. About the Theory of so-called Adsorption of Soluble Substance. *Kungliga Svenska Vetenskapsakademiens. Handlingar* **1898**, *24* (4), 1–39.

(38) Ho, Y. S.; McKay, G. A Comparison of Chemisorption Kinetic Models Applied to Pollutant Removal on Various Sorbents. *Trans IChemE* **1998**, *76* (Part B), 332–340.

(39) Weber, W. J.; Morris, J. C. Kinetics of Adsorption on Carbon from Solution, in Proceeding of the American Society of Civil Engineers. *J. Sanit. Eng. Div.* **1963**, *89* (SA2), 31–59.

(40) Langmuir, I. The Constitution and Fundamental Properties of Solids and Liquids. Part I. Solids. *J. Am. Chem. Soc.* **1916**, *38*, 2221–2295.

(41) Freundlich, H. M. F. Over the Adsorption in Solution. *Z. (J. Phys. Chem.)* **1906**, *57*, 385–470.

(42) Pokhrel, D.; Viraraghavan, T. Arsenic Removal from an Aqueous Solution by Modified A. Niger Biomass: Batch and Isotherm Studies. *J. Hazard. Mater.* **2008**, *150*, 818–825.

(43) Atkins, P.; de Paula, J. *Atkin's Physical Chemistry*; 8th ed.; Oxford University Press: Oxford, 2006.

(44) Thomas, W. J.; Crittenden, B. *Adsorption Technology and Design*; Butterworth-Heinemann: Oxford, 1998.

Received for review November 10, 2008. Accepted April 12, 2009. The University Grants Commission (New Delhi), India, has supported this work financially.

JE900282M